

1965).

<sup>4</sup>A. I. Burshtein, *Lektsii po kursu Kvantovaya kinetika (Quantum Kinetics Lecture Course)*, Pt. 1, Novosibirsk State Univ., 1968, p. 23.

<sup>5</sup>A. Ashkin, *Phys. Rev. Lett.* **25**, 1321 (1970).

<sup>6</sup>A. P. Kazantsev, *Zh. Eksp. Teor. Fiz.* **63**, 1628 (1972); **66**, 1599 (1974) [*Sov. Phys. JETP* **36**, 861 (1973); **39**, 784 (1974)]; *Pis'ma Zh. Eksp. Teor. Fiz.* **17**, 212 (1973) [*JETP Lett.* **17**, 150 (1973)].

<sup>7</sup>A. P. Kazantsev and G. I. Surdutovich, *Pis'ma Zh. Eksp. Teor. Fiz.* **21**, 346 (1975) [*JETP Lett.* **21**, 158 (1975)].

<sup>8</sup>A. P. Kazantsev, *Zh. Eksp. Teor. Fiz.* **67**, 1660 (1974) [*Sov.*

*Phys. JETP* **40**, 825 (1975)].

<sup>9</sup>A. P. Botin and A. P. Kazantsev, *Zh. Eksp. Teor. Fiz.* **68**, 2075 (1975) [*Sov. Phys. JETP* **41**, 1038 (1975)].

<sup>10</sup>A. Yu. Pusep, *Zh. Eksp. Teor. Fiz.* **70**, 851 (1976) [*Sov. Phys. JETP* **43**, 441 (1976)].

<sup>11</sup>V. M. Fain, *Fotony i nelineinye sredy (Photons and Nonlinear Media)*, *Sov. Radio*, 1972, p. 113.

<sup>12</sup>A. Abragam, *Principles of Nuclear Magnetism*, Oxford, 1961, (Russ. Transl. III, 1963, p. 32).

Translated by J. G. Adashko

## New bands in low-temperature fluorescence of anthracene crystals at high exciton concentrations

V. A. Benderskiĭ, V. M. Beskrovnyi, V. Kh. Brikenshtein, V. L. Broude,<sup>1)</sup> A. G. Lavrushko, and A. A. Ovchinnikov<sup>2)</sup>

*Division of Institute of Chemical Physics, USSR Academy of Sciences*

(Submitted July 14, 1976)

*Zh. Eksp. Teor. Fiz.* **72**, 106–118 (January 1977)

Changes in the fluorescence spectra of the anthracene crystals were investigated at a pulsed pump intensity  $10^{20}$ – $2 \times 10^{23}$  cm<sup>-2</sup> sec<sup>-1</sup> and at crystal temperatures (at the instant of measurement) 10–16° K. It is observed that at exciton concentrations  $(2\text{--}5) \times 10^{17}$  cm<sup>-3</sup> each of the vibronic bands of the fluorescence spectrum acquires, above a certain threshold, an additional component with half-width 100–150 cm<sup>-1</sup>. At maximum pump intensities the additional emission can reach half the total integrated emission of the crystal. When the new bands are produced, a decrease is observed in the quantum yield of the total radiation from the crystal. It is shown that these bands are due to interaction between the excitons when their concentration is high. This interaction is interpreted in terms of a phase transition with formation of a new phase having an increased exciton concentration. Experimental and theoretical estimates are obtained for the exciton concentration in the phase, and yield values that are one or two orders of magnitude smaller than the concentration of the molecules in the crystal.

PACS numbers: 78.55.Kz, 71.35.+z

### 1. INTRODUCTION

An investigation of germanium crystals subjected to intense optical excitation has led to observation of exciton condensation, as a result of which electron-hole drops (EHD) are produced at a definite temperature and concentration of the excitons<sup>[1–3]</sup>; this process has a threshold. Data on the formation of EHD in crystals of other semiconductors were also obtained.<sup>[4,5]</sup> For a gas of Frenkel excitons, the binding energies of which are much larger than their interaction energies, one can expect condensation to result not in EHD but in drops of a dielectric exciton liquid. Because of the short-lived interaction (compared with the Coulomb interaction) between small-radius excitons, and also because of their short lifetimes, the exciton concentrations needed for this purpose must be several orders of magnitude higher than in semiconducting crystals, and the measurement times correspondingly shorter. It was observed earlier<sup>[6]</sup> that in a molecular anthracene crystal a strong broadening of the exciton-fluorescence bands sets in at exciton concentrations  $\sim 10^7$  cm<sup>-3</sup>. This phenomenon was tentatively explained as being due to formation of a dielectric exciton phase of increased density, the emission of which consists of broad bands that

are superimposed on the narrower fluorescence bands of the free excitons.

An investigation of the fluorescence of anthracene crystals at low temperatures and high optical-pumping levels<sup>[7–9]</sup> has shown that, depending on the experimental conditions (sample thickness, dimensions of the pumping region, the quality of the end-face faceting) the result is either lasing at the most intense vibronic transition in the fluorescent spectrum, or a decrease of the fluorescence quantum yield as a result of bimolecular recombination of the excitons (nonlinear quenching). Since lasing is accompanied by stabilization of the exciton concentration, high concentrations can be obtained only by suppressing the lasing, in particular, by decreasing the linear dimensions of the pumped volume. Even in this case, however, the exciton concentration increases sublinearly with the pump, owing to nonlinear quenching, making it necessary to use very high pump levels (up to  $10^{23}$  cm<sup>-2</sup> sec<sup>-1</sup>) in order to exceed the threshold exciton concentrations at which the aforementioned band broadening takes place. Under these conditions, heating of the crystals during the pulse is unavoidable because of the nonradiative conversion of the excitation quanta into excitons of the lowest band and the release

of heat during the nonlinear quenching. Since the crystal heating is itself accompanied by a broadening of the fluorescence-spectrum bands, a major difficulty in the experiment is the separation of effects due to sample heating, on the one hand, and to increase of the exciton concentration, on the other. In addition, the broadening of the fluorescence bands can be due also to the deformation that the pulsed heating introduces in the pumped region of the crystal. Finally, the observed change in the shapes of the spectrum bands may be due to reversible accumulation of photochemical defects, nonequilibrium phonons, or excitons, which occur in nonradiative transitions, or which are produced either under the influence of the pump, or when the excitons recombine.

In view of the foregoing, we describe in the first half of the present article special experiments that make it possible to obtain the required discrimination, i. e., to demonstrate that the observed effects are due to increased exciton concentration and not to extraneous phenomena such as heating, etc. In the second half of the paper we describe methods of separating the "phase" spectrum from the combined emission of the crystal, we analyze the regularities observed in this emission, and present certain theoretical derivations and estimates.

## 2. EXPERIMENTAL PROCEDURE

The setup for the investigation of the fluorescence spectra in the nanosecond emission range and at helium temperatures was described earlier.<sup>[9]</sup> The optical pumping was with a pulsed nitrogen laser ( $\lambda = 337.1$  nm) with duration 8 nsec at pulse half-width and a repetition frequency 100 Hz.

We used sublimated single-crystal anthracene plates. Since perfect anthracene crystals have a high thermal diffusivity at low temperatures (the phonon mean free path exceeds  $30 \mu$  at a velocity  $10^5$  cm/sec<sup>[10]</sup>), we used, to obtain high exciton concentrations at the lowest possible temperature, relatively thick samples in which heat could still be drained from the pumped surface region into the interior during the measurement time (during the pump pulse). At the indicated phonon velocity and pulse duration, the required crystal thicknesses were 10–20  $\mu$ . In thinner samples, owing to the small volume, the temperature turned out to be higher at the end of the pulse. The samples returned to the original temperature in the intervals between the pulses ( $10^{-2}$  sec) via heat transfer to the thermostat bath, characterized by a time on the order of  $10^{-5}$  sec.<sup>[10]</sup>

The absorption coefficient was  $4 \times 10^{-4}$  cm<sup>-1</sup> when the laser beam was polarized along the *b* axis of the crystal, and  $2 \times 10^4$  cm<sup>-1</sup> in case of polarization along the *a* axis.<sup>[11]</sup> Since the laser beam cross section was not uniform, a special system of slits and lenses<sup>[9]</sup> at the entry to the monochromator was used to focus the light from a selected section of the sample (dimension 0.1  $\times$  0.1 mm) within which the inhomogeneity of the pump did not exceed 10%. From an analysis of the shapes of the fluorescence-damping curves at low pump levels

( $< 10^{20}$  cm<sup>-2</sup> sec<sup>-1</sup>) we determined the exciton lifetimes,  $3.5 \pm 0.5$  nsec in the interval 6–40° K.

It should be recalled that, owing to the use of a stroboscopic procedure,<sup>[9]</sup> each measured point was the result of statistical averaging over  $10^3$  pump pulses. Therefore any spectrum-distortion accumulation that was irreversible in a time less than  $10^{-2}$  sec, should have been accompanied by irreversibility in prolonged measurements. Since no violations of reproducibility were observed in the measurements, we shall analyze in the following explanation of the phenomena only rapid processes in which the initial state of the sample is restored in the interval between the pulses.

## 3. THE FIRST EXPERIMENT

In our earlier studies<sup>[6]</sup> we monitored the sample temperature with a "tetracene thermometer"<sup>[10]</sup> based on the measurements of the Debye-Waller factor in the fluorescence spectrum of a tetracene impurity introduced into the crystal. An important advantage of this thermometer is absence of inertia, so that the temperature can be measured at any instant of time during the pump pulse. The accuracy of the method, however, is doubtful, for in view of the finite rate of propagation of the heat into the interior of the sample the anthracene fluorescence can become reabsorbed by a tetracene impurity located in the still-unheated region of the crystal. The "tetracene thermometer" then underestimates the temperature. To monitor this circumstance and to obtain more correct values of the temperature of the pump region, a thin crystal layer with  $\sim 10^{15}$  cm<sup>-3</sup> tetracene impurity was grown additionally on the surface of the pure crystal. The thickness of the impurity layer (0.3–0.4  $\mu$ ) was such that the pump light, polarized along the *a* axis, was absorbed in it almost uniformly. Figure 1 shows the dependence of the temperature in this layer on the pump intensity at the pump-pulse maximum. It shows also the temperatures measured in a sample of the same thickness but with uniform distribution of the tetracene impurity over the volume. It is seen that in the second case the readings of the "tetracene thermometer" are indeed too low. The results obtained with the additionally grown layer were compared with the known data on the temperature dependence of the heat content of the anthracene crystal.<sup>[12]</sup> To this end we subtracted from the pump values the amount of heat delivered to the crystal. Account was taken of the dependence of the pump quenching factor, which determines the absorbed-energy fraction going into heat and into fluorescence. The temperature was then determined in accordance with the data of<sup>[12]</sup>. This result is also shown in Fig. 1. It is seen that it agrees well with the dependence obtained for the sample with the additional layer, thus confirming the accuracy of the temperature measurement in the layer with the "tetracene thermometer."

Following these measurements, the samples with the additional layer were used to obtain the fluorescence spectra of the anthracene crystal at high pump levels. These spectra were then compared with the spectra obtained by exciting with an ordinary mercury lamp (very

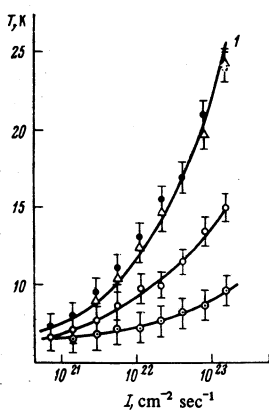


FIG. 1. Temperature of illuminated layer of anthracene crystal vs the intensity of the exciting light: curve 1 shows the calculated heating of a crystal  $d = 10^{-3}$  cm at the instant of time corresponding to the maximum pump pulse ( $t_p = 10$  nsec);  $\Delta$ —temperature under a phthalocyanine layer, determined by measuring the shape of the fluorescent spectrum of anthracene;  $\bullet$ —temperature measured with a “tetracene thermometer” in a surface layer;  $\circ$ —readings of “tetracene thermometer” when the impurity is uniformly distributed over the sample in a crystal of the same thickness;  $\odot$ —readings of “tetracene thermometer” when the impurity is uniformly distributed in a crystal  $5 \times 10^{-3}$  cm thick.

low pump level), but at thermostat-bath temperatures maintained at the values corresponding to the readings of the “tetracene thermometer” in the surface layer under intense pumping. Under these conditions we have confirmed the previously observed<sup>[6]</sup> fact that the fluorescence bands of strongly excited anthracene are subject to a broadening in excess of the temperature broadening.<sup>3)</sup>

#### 4. SECOND EXPERIMENT

In the preceding experiments one could not exclude the possibility that part of the energy fed to the crystal by the pulsed heating went to deform the crystal, thus causing band broadening other than thermal. To eliminate this factor, the following experiment was performed. The fluorescence spectra pertaining to identical optical pump levels but to different resultant exciton concentrations were compared by depositing, by vacuum sublimation, a thin ( $\sim 0.1 \mu$ ) layer of organic dye, copper phthalocyanine, on part of the crystal surface. This layer had a noticeable absorption and attenuated the pump-light intensity by a factor 30–40.

The control samples were simultaneously doped with tetracene in an amount such that the crystal was heated to the same degree when excited either through the dye layer or on the free part of the surface. The exact values of this heat rise (see Fig. 1) were determined from the fluorescence spectrum of the anthracene excited through the dye layer, and this spectrum was temperature-calibrated beforehand for this purpose.

In this series of experiments we compared the fluorescence spectra of the anthracene in uncoated crystal-surface sections and those coated with a phthalocyanine layer. The results of this comparison are shown in

Fig. 2 and confirm the presence of an appreciable broadening in excess of the thermal broadening. We note that the depositing of the dye does not disturb the crystal surface-layer quality, as evidenced by the absence of changes in the anthracene fluorescence spectra at low excitation levels before and after the coating.

These experiments have confirmed directly that the anthracene fluorescence broadening in excess of the thermal broadening, under intense pumping, is due to the increase in the exciton concentration. In addition, the same experiments allow us to reject the assumption that the fluorescence band shape is influenced by the pulsed character of the heating and that impact deformation of the sample takes place as a result of this heating.

#### 5. THIRD EXPERIMENT

The second measurement method described above does not show whether the observed changes in the band shape can be affected by photochemical defects, non-equilibrium phonons, or excitons produced when the optical excitation is relaxed or produced under the influence of the pump. We have therefore performed the following experiment:

The anthracene crystal was excited by focusing on its surface a strip of light a fraction of a millimeter wide and up to 5 mm long. Under these conditions, lasing was produced in the crystal on the  $23692 \text{ cm}^{-1}$  vibronic band of the anthracene fluorescence spectrum.<sup>[7–9]</sup> The exciton concentration was stabilized at a level that could be determined from the intensity of the remaining bands of the spectrum. Then, without changing the excitation intensity, the length of the strip was decreased with a diaphragm to 0.1–0.2 mm. This suppressed the generation of light and increased the exciton concentration by 2.5–3 times. At the same time a change in band shape similar to that shown in Fig. 2 was observed.

These experiments allow us to state that the observed

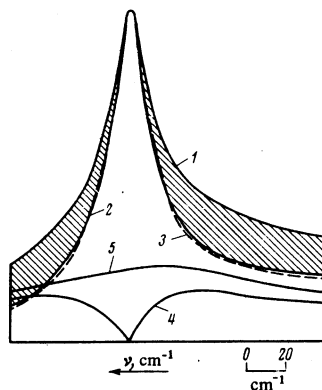


FIG. 2. Determination of the fraction of the new emission in the fluorescence spectrum of an anthracene crystal at a high level of optical pumping: 1— $1403 \text{ cm}^{-1}$  0–0 band at  $I_0 = 1.5 \times 10^{23} \text{ cm}^{-2} \text{ sec}^{-1}$  and at an illuminated-layer temperature  $T = 22.5^\circ \text{K}$  ( $t_p = 10$  nsec); 2—the same band at  $I_0 = 10^{20} \text{ cm}^{-2} \text{ sec}^{-1}$  and  $T = 22.5^\circ \text{K}$ ; 3—shape of band under the phthalocyanine layer at  $I_0 = 1.5 \times 10^{23} \text{ cm}^{-2} \text{ sec}^{-1}$ ; 4—determination of the fraction of the new band by the first method; 5—determination of the fraction of the new band by the second method.

changes in the fluorescence spectrum are indeed not caused by the interfering factors mentioned above, but are due exclusively to the change of the exciton concentration in the sample, i.e., to interaction of the Frenkel excitons when their concentration is high.

## 6. SEPARATION AND ANALYSIS OF THE NEW EMISSION OF THE ANTHRACENE CRYSTALS

Quantitative information on the character and parameters of the crystal emission in excess of the temperature-induced emission can be most conveniently obtained by using the procedure of the second experiment, although the two other series of experiments also agreed fully with this information.

Figure 2 shows the changes in the shape of the 23692  $\text{cm}^{-1}$  vibronic transition band when the exciton concentration is changed by approximately 30–40 times. These changes are typical also of two other vibronic bands of the fluorescence spectrum of anthracene. In this figure, the two bands obtained by applying the excitation through a dye layer and to the free part of its surface were equalized in intensity at the maximum of the band.

It was shown above that the additional broadening illustrated in Fig. 2 is due to exciton–exciton interactions. It can therefore be caused either by exciton–exciton collisions, which broaden the exciton bands of the fluorescence spectrum, or to superposition of the exciton bands on the bands corresponding to formation of a bound state of excitons. The first cause should apparently be excluded, since the exciton–exciton collisions cannot lead to the threshold-dependent change in the fluorescence quantum yield, which will be described below (see Fig. 5), or to the kinetic characteristics of the emission (see Fig. 6). The analysis that follows is therefore based on the assumption of two components of the combined-fluorescence bands.

The principal parameter in this case is the share of the new emission in the combined total spectrum; this share is determined by methods described below, which do not claim to determine the shape of the bands of the new emission. The first method was based on

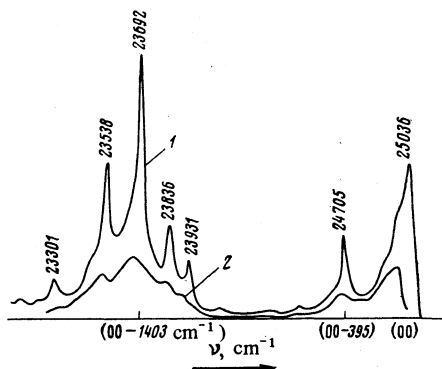


FIG. 3. Fluorescence spectrum of anthracene crystal at high pump intensity ( $I_0 = 1.5 \times 10^{23} \text{ cm}^{-2} \text{ sec}^{-1}$ ,  $T = 22.5^\circ\text{K}$ ,  $t_p = 10 \text{ nsec}$ ): 1—total spectrum, 2—spectrum of new emission (separated by the second method).

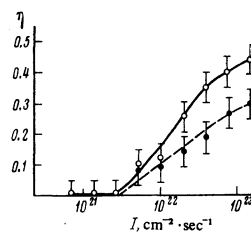


FIG. 4. Dependence of the relative fraction  $\eta$  of the new emission on the excitation intensity  $I$  (the measurements were performed at a constant temperature of the illuminated layer  $T = 22.5^\circ\text{K}$ ; to this end the thermostat-bath temperature was increased when the pump intensity was decreased in such a way that the fluorescence bands of the anthracene under the phthalocyanine layer retained the same shape;  $t_p = 10 \text{ nsec}$ ,  $d = 10^{-3} \text{ cm}$ ): ●—reduction by the first method, ○—reduction by the second method.

direct subtraction of the bands with their intensities equalized at the maximum. In this case the difference band is a double-hump curve with zero amplitude at the maximum of the initial bands. This, naturally, underestimates the fraction of the new emission in the combined band. Another way of separating the bands is to multiply the subtracted band by a factor such that the new-emission band is smoothed out and has a single maximum.

As a measure of the non-temperature broadening, we introduce the parameter  $\eta$ , which corresponds to the fraction of the new emission in the total emission of the crystal in the region of the investigated band,  $\eta = (S - S_0)/S$ , where  $S$  and  $S_0$  are the areas of the bands at high and low exciton concentrations. Although the values of  $\eta$  determined by the two separation methods differ by approximately 1.5 times, the dependences of  $\eta$  on the pump intensity and on the temperature turn out to be similar.

The sensitivity of the apparatus (the signal to noise ratio was approximately 40) made it possible to determine values of  $\eta$  as low as 0.05. This quantity determines the accuracy with which the threshold of the effect is determined.

Figure 3 shows the fluorescence spectrum of the anthracene crystal (the time position of the pulse maximum) at the pump maximum, the value of which was limited by the sample surface-damage threshold. The figure shows also the new-emission spectrum separated by the described procedure. It is seen that each of the vibronic bands in this spectrum corresponds to a broader band (half-width 100–150  $\text{cm}^{-1}$ ) of new emission, which is possibly slightly shifted (20–30  $\text{cm}^{-1}$ ) in the long-wave direction. The values of  $\eta$  are approximately the same for all the vibronic bands.

Figure 4 shows the dependence of  $\eta$  on the pump intensity for two band-separation methods. A characteristic feature is the presence of a threshold pump intensity ( $\sim 3 \times 10^{21} \text{ cm}^{-2} \text{ sec}^{-1}$ ), corresponding to an exciton concentration  $2 \times 10^{17} \text{ cm}^{-3}$  (this value lies in the range  $(2-5) \times 10^{17} \text{ cm}^{-3}$  for different crystals). The maximum values of  $\eta$  corresponding to a pump  $10^{23}$

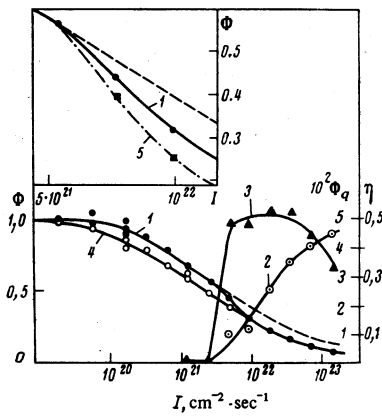


FIG. 5. Plots of the fluorescence quantum yields  $\Phi$  against the intensity of the exciting light  $I$ : 1 (●)—nonlinear-quenching curve of the integrated (over the spectrum) fluorescence of the anthracene, measured at a constant illuminated-layer temperature  $T = 22.5^\circ\text{K}$  (the procedure used to maintain the temperature constant is indicated in the caption of Fig. 4). The theoretical curve<sup>[13]</sup> is shown dashed; 2 (○)—dependence of the fraction  $\eta$  of the new emission on the excitation intensity; 3 (▲) quantum yield  $\Phi_q$  of the new emission; 4 (○) nonlinear quenching curve at  $T = 60^\circ\text{K}$ ; 5 (■)—exciton-emission quantum yield calculated from curves 1 and 2.

$\text{cm}^{-2} \text{sec}^{-1}$  range from 0.4 to 0.5 for different crystals.

When new bands appear, the total quantum yield of the anthracene fluorescence  $\Phi = \Phi_e + \Phi_q$  is decreased ( $\Phi_e$  is the exciton-emission quantum yield and  $\Phi_q$  is the quantum yield of the new emission). This is shown in Fig. 5, which gives also the changes of  $\Phi_e$  and  $\Phi_q$  obtained by separating the spectra ( $\Phi_q = \eta\Phi$ ). The values of  $\Phi_q$  for different samples amount to  $(3-6) \times 10^{-2}$ . A 10–20% decrease of  $\Phi_q$  is observed at  $I_0 > 5 \times 10^{22} \text{cm}^{-2} \text{sec}^{-1}$ .

With increasing temperature,  $\eta$  decreases. At  $I_0 \approx 2 \times 10^{23} \text{cm}^{-2} \text{sec}^{-1}$  the effect is not observed at  $T > 50^\circ\text{K}$ , and under weaker pumping the new emission vanishes at lower temperatures. If it is assumed that the threshold exciton concentration is proportional to  $\exp(-\epsilon/kT)$ , then the range of  $\epsilon$  is 40–60  $\text{cm}^{-1}$ . It should be noted that at  $T > 50^\circ\text{K}$ , when no new emission is observed, there is likewise no break on the nonlinear-quenching curves.

The kinetic characteristics of the total, exciton, and new emissions are given in Fig. 6. The new emission appears after a threshold exciton concentration is produced, in agreement with the previously noted<sup>[6]</sup> lag between the changes in the spectrum and the rise of the pump pulse. On the decreasing part of the pulse, the new emission is preserved at lower values of the pump intensity. Thus, a unique hysteresis is observed, and the same pump value corresponds to different values of  $\eta$ .

## 7. DISCUSSION OF RESULTS

The fact that the observed new emission is found to be explicitly connected with the increased exciton concentration in the crystal, as well as the threshold char-

acter of the appearance of this emission, can serve as the basis for the interpretation of the phenomenon as a phase transition in a system of Frenkel excitons, with formation of a two-phase system. An important argument in favor of the exciton condensation is the decrease of the quantum yield of the fluorescence of the crystal when new emission is produced, inasmuch as the nonlinear quenching of the excitons should accelerate in the denser phase.

We start with this assumption and consider the growth kinetics of the exciton phase with the increased density. The exciton mean free path in anthracene crystals at medium temperatures decreases rapidly with increasing temperature, and does not exceed 100 Å in the range 15–40°K. Inasmuch as the exciton mean free path is comparable with or smaller than the proposed drop radius  $R$ , the rate of exciton capture by the drop is described in the diffusion approximation. The equations for the concentrations  $n$  of the free excitons and for the total number of excitons in the drop (i.e., for the radius  $R$  of a drop in which the exciton concentration  $n_d$  is constant) differ from the case of production of EHD in germanium, when  $\lambda > R$ ,<sup>[1]</sup> and take the form

$$\frac{dn}{dt} = I_0 - \frac{n}{\tau} - K_{SS}n^2 - 4\pi DRN(n - n_0), \quad (1)$$

$$\frac{d}{dt} \left( \frac{4}{3} \pi R^3 n_d \right) = 4\pi DR(n - n_0) - \frac{4\pi}{3} R^2 \frac{n_d}{\tau_d}, \quad (2)$$

where  $D$  is the exciton diffusion coefficient,  $N$  is the drop concentration,  $n_0$  is the threshold concentration of the free excitons and corresponds to the start of condensation,  $\tau$  is the radiative lifetime of the free excitons,  $\tau_d$  is the lifetime of the excitons in the drop (it includes the radiative and nonradiative channels, the latter being determined by the collision annihilation of the excitons at constant  $n_d$ ), and  $K_{SS}$  is the constant of bimolecular concentration of the free excitons.

From the solution of (2) we obtain under stationary conditions

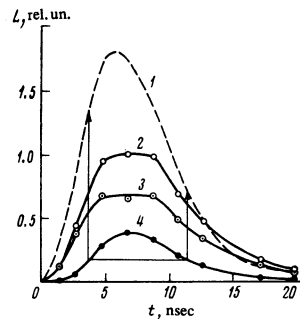


FIG. 6. Time dependences of the fluorescence at a high pump intensity  $I_0 = 1.0 \times 10^{23} \text{cm}^{-2} \text{sec}^{-1}$ . The measurements were made at a constant illuminated-layer temperature  $T = 24^\circ\text{K}$ , corresponding to the temperature at the end of the optical-pumping pulse, and the procedure used to maintain the temperature constant is indicated in the caption of Fig. 4. 1—optical-pumping pulse (scale decreased by a factor 5); 2 (○)—total emission; 3 (○)—emission of free excitons; 4 (●)—“phase” emission.

$$R = \left[ 3D\tau_d \frac{n-n_0}{n} \right]^{1/2}. \quad (3)$$

The equation for the concentration of the free excitons then takes the form

$$\alpha z^2 + \beta z^3 + (2\alpha + 1)z = H - \alpha - 1, \quad (4)$$

where

$$z = \frac{n}{n_0} - 1, \quad H = \frac{I_0\tau}{n_0}, \quad \alpha = K_{ss}n_0\tau, \quad (5)$$

$$\beta = 4\pi(3D^3\tau^2\tau_d)^{1/2} N \left( \frac{n_0}{n_d} \right)^{1/2}.$$

The pump threshold is equal to

$$H_0 = 1 + \alpha, \quad (6)$$

and the condensation in accordance with (4) can take place under the condition  $\beta \gg \alpha$ . The phase emission, equal to the phase flux ( $\beta z^{3/2}$ ) multiplied by the quantum yield  $\Phi_q$  of its emission at pump value near threshold ( $z \ll 1$ ,  $H \approx H_0$ ), is given by

$$L_q = \Phi_q \frac{\beta}{(1+2\alpha)^{1/2}} (H - H_0)^{3/2}, \quad (7)$$

while in the region  $H \gg H_0$ ,  $z \gg 1$  we have

$$L_q = \Phi_q H. \quad (8)$$

With further increase of the pump, the rate of bimolecular quenching catches up with the rate of the influx of the excitons into the phase, as a result of which  $L_d$  begins to decrease. This behavior of  $L_q$  agrees qualitatively with the experimental data. Figure 7 shows plots of  $\Phi_e$ ,  $\Phi_q$ , and  $\eta$  against  $H$ , calculated from (2) and (4) at  $\alpha = 3$  and  $\beta = 10$ ; they agree satisfactorily with the experimental data of Fig. 5. If it is assumed that the radiative lifetime of the excitons does not change during condensation, then the value of  $\tau_d$  is given by  $\Phi_q\tau = (1-2) \times 10^{-19}$  sec. It is important that the values  $\beta/\alpha \approx 10$  and  $R \gtrsim 10^{-6}$  cm at  $z \geq 1$  correspond to reasonable values of the unknown parameters, namely  $N = 10^{14} - 10^{15}$  cm $^{-3}$  and  $n_0/n_d = 10^{-2} - 10^{-3}$  (we used in the calculations the values of  $n_0$ ,  $\tau$ , and  $\tau_d$  given above, as well as  $K_{ss} = 3 \times 10^{-9}$  cm $^3$  sec $^{-1}$  [8] and  $D = 1$  cm $^2$  sec $^{-1}$ ). Thus, a reduction of the data of Fig. 5 within the framework of the assumption of production of an exciton phase of increased density shows that, as a result of the short lifetimes and the short diffusion length of the free excitons, only minute droplets of the exciton phase can be produced, containing  $\sim 10^2 - 10^3$  excitons, the exciton concentration in the drops being much lower than the concentration of the molecules in the anthracene crystal ( $2 \times 10^{21}$  cm $^{-3}$ ).

The data of Fig. 6 show that the exciton concentrations at which drops are produced are several times larger than those at which they vanish. This can be attributed to the supersaturation, which is a characteristic of formation of the new phase. The value of the supersaturation, determined by the mechanism that produces the condensation nucleus, depends in this case also on

the mechanism whereby the drops vanish, in which, possibly, an important role is played by the heat released from the drop as a result of the high rate of nonradiative annihilation of the excitons in the drop.

We examine now in greater detail the conditions for the formation and possible concentration of the excitons in the condensed phase. The Hamiltonian of the lattice gas of Frenkel excitons can be represented in the form

$$\hat{\mathcal{H}} = \sum_{n,m} b_n^+ b_m T_{nm} + \frac{1}{2} \sum_{n,m} b_n^+ b_n b_m^+ b_m V_{nm}, \quad (9)$$

where  $b_n^+$  and  $b_n$  are the Pauli operators for exciton production and annihilation, the summation being extended over the entire lattice,  $T_{nm}$  are the exciton transport integrals in the lattice, and  $V_{nm}$  is close to the difference between the van der Waals energies of two excited molecules, on the one hand, and of a pair of molecules of which only one is excited, on the other, since the exciton-exciton interaction with participation of phonons and the additional interaction connected with the resonant transfer of two excitons to a single center are apparently small.

Since the considered temperatures are higher than the Bose-condensation temperature, it might seem at first glance that classical statistical-mechanics approach is sufficient. However, the exciton wavelength at the temperature of the experiment is comparable with the exciton-exciton scattering length. The dynamics of the exciton-exciton interaction has therefore a quantum-mechanical character. Consequently, we can consider values of  $T$  and  $V$  such that there is no bound state of the two excitons, but, as will be shown below, the existence of large exciton aggregates is possible.

The energy of the state  $N$  of the noninteracting excitons situated at the bottom of the exciton band is

$$\mathcal{E}_0 = -2N \sum_i T_i = -6N\bar{T}, \quad (10)$$

and the energy of a certain number of closest-packed excitons having zero kinetic energy (if we disregard surface effects, as is permissible at large  $N$ ) is equal to

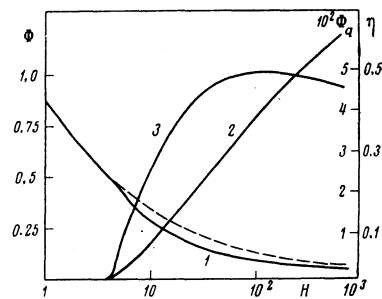


FIG. 7. Calculated plots (at  $\alpha = 3$  and  $\beta = 10$ ) for the exciton emission  $\Phi_e$  (curve 1), the fraction of the new emission  $\eta$  (curve 2), and the quantum yield of the new emission  $\Phi_q$  (curve 3) as functions of the pump intensity.

$$\mathcal{E}_i = -N \sum_i V_i = -3N\bar{V}. \quad (11)$$

Consequently, at

$$2\bar{T} > \bar{V} \quad (12)$$

there exists an exciton condensed state with an energy lower than that of the exciton gas. Of course, the density of the minimum-energy state is not necessarily maximal, for in this case the loss of kinetic energy may turn out to be very large. It should be noted, however, that in the one-dimensional case, where exact solutions exist for a system of paulions<sup>[13]</sup> the dense state has a maximum density for large  $N$  if the condition (12) is satisfied. For the three-dimensional case, this problem is much more complicated in the presence of anisotropy.

We shall show below that the exciton phase can have a low equilibrium concentration (in comparison with the concentration of the molecules in the crystal). The estimate can then be obtained by considering a system of hard spheres<sup>4)</sup> satisfying Bose statistics at not too high a concentration. According to<sup>[16]</sup>, at  $T=0$  the free energy of a system of spheres having a radius  $d$  and a concentration  $\rho$  is equal to

$$f_- = \frac{\pi d}{m} \rho^2 (1 + 1.5 \rho^h d^h). \quad (13)$$

The average attraction energy in this state (when the wave function is approximated by the classical function for a system of hard spheres) is equal to

$$f_+ = -3\bar{V}d^3\rho^2. \quad (14)$$

The foregoing expression is the first term of the expansion in the small density, while the next term is of order  $\rho^3$ , so that the retention of the  $\rho^{5/2}$  term in (13) is legitimate. Expressing the effective mass  $m^*$  in terms of the parameters of the Hamiltonian ( $1/m^* = 2\bar{T}d^2/\hbar^2$ ) and minimizing the total energy of the system  $f = f_+ + f_-$ , we obtain the concentration  $\rho^*$  corresponding to the minimum of the energy of the spheres in the system<sup>5)</sup>:

$$\rho^* = \frac{144}{225\pi^2} \rho_0 \left( \frac{\bar{V}}{\bar{T}} - \frac{2\pi}{3} \right)^2, \quad (15)$$

where  $\rho_0$  is the maximum exciton concentration. The energy of this state relative to the bottom of the exciton band is equal to  $\delta = 6\bar{V}\rho^*/\rho_0$ . Since the last quantity corresponds to a shift of the new bands relative to the exciton bands and should lie within the limits of the width of the experimentally observed new bands, we assume that  $\delta = 10 - 10 \text{ cm}^{-1}$ . We then obtain from (15)  $\rho^*/\rho_0 = 0.01 - 0.1$ . The obtained value of  $\rho^*/\rho_0$  agrees with the estimate given above for  $n_0/n_d$  and obtained from the analysis of the kinetic data.

## 8. CONCLUSION

The foregoing analysis of the experimental material and some theoretical estimates show that a condensed

exciton phase with a concentration smaller by one or two orders of magnitude than the concentration of the molecules in the crystal is produced in anthracene crystals at high exciton concentrations and at low temperatures. The radiation from this phase can be as much as one-half the total radiation of the crystal under these conditions.

Presented simple estimates of the parameters of this phenomenon do not take into account some undoubtedly important details, such as the anisotropy of the motion of the excitons in the anthracene crystal, or the role of the exciton-impurity complexes. In particular, the condensation process must be strongly anisotropic, since the motion of the excitons in anthracene crystals at helium temperatures is in fact close to one-dimensional (along the  $\mathbf{a}$  axis), because the band with large effective mass is not analytic along the  $\mathbf{c}'$  axis.<sup>[14b]</sup> On the other hand, in the  $(\mathbf{bc}')$  plane, where the kinetic energy of the excitons is low, the conditions for their binding should be the most favorable. However, although these features of the anthracene crystals are not taken into account, we can draw rather reliable conclusions, for example that there is no connection between the observed phenomena and biexciton formation or exciton-exciton collisions in the gas of free excitons. This conclusion is based on the assumptions that neither of these effects can have a threshold or cause the experimentally observed change of the nonlinear quenching curves and the hysteresis in the kinetics of the new emission. One cannot deny, of course, the possible effect of exciton-exciton collisions on the type of the condensate band and, in particular, the connection between this process and the observed large widths of the bands.

The circumstances under which Frenkel excitons condense in anthracene crystals call for additional research. The measurements made at lower temperatures, owing to the decreased pump-pulse duration and the increased absorption coefficient over its wavelength (in the latter case the concentration of the excitons increases while the temperature of the illuminated layer remains constant) will be the subject of our forthcoming studies.

The authors thank É. I. Roshba for a useful discussion of the experiments.

<sup>1)</sup>Institute of Solid State Physics, USSR Academy of Sciences.

<sup>2)</sup>L. Ya. Karpov Physico-Chemical Research Institute.

<sup>3)</sup>In the earlier experiments<sup>[6]</sup> the tetracene impurity was uniformly distributed in the volume, but the temperature maintained in the crystal corresponded to the end of the pump pulse, when a crystal  $10 \mu$  thick is heated practically uniformly. Under these conditions, the "tetracene thermometer" produces undistorted readings and the data obtained in<sup>[6]</sup> on the time variation of the band half-width are qualitatively correct.

<sup>4)</sup>See<sup>[14a]</sup> concerning the possibility of reducing the problem of a system of excitons to the problem of impermeable particles.

<sup>5)</sup>It is seen from (15) that a dense state is realized under the condition  $\bar{V}/\bar{T} < 2\pi/3$ , which is close to (12).

<sup>1)</sup>L. V. Keldysh, in: Éksitony v poluprovodnikakh (Excitons in Semiconductors), Nauka, 1971, p. 5; V. S. Bagaev, N. V. Zamkovets, L. V. Keldysh, N. N. Sibel'din, and V. A.

- Tsvetkov, Zh. Eksp. Teor. Fiz. **70**, 1501 (1976) [Sov. Phys. JETP **43**, 783 (1976)].
- <sup>2</sup>Ya. E. Pokrovskii and K. I. Svistunova, Fiz. Tekh. Poluprovodn. **4**, 491 (1970) [Sov. Phys. Semicond. **4**, 409 (1970)].
- <sup>3</sup>J. P. Wolfe, W. L. Hansen, E. E. Haller, R. S. Markiewicz, C. Kittel, and C. D. Jeffries, Phys. Rev. Lett. **34**, 1292 (1975).
- <sup>4</sup>Ya. Pokrovskii, Phys. Status Solidi **11**, 385 (1972).
- <sup>5</sup>V. G. Lysenko, V. I. Revenko, T. G. Tratas, and V. B. Timofeev, Zh. Eksp. Teor. Fiz. **68**, 335 (1975) [Sov. Phys. JETP **41**, 163 (1975)].
- <sup>6</sup>V. A. Benderskii, V. Kh. Brikenstein, V. L. Broude, and I. I. Tartakovskii, Pis'ma Zh. Eksp. Teor. Fiz. **22**, 332 (1975) [JETP Lett. **22**, 156 (1975)].
- <sup>7</sup>V. A. Benderskii, V. Kh. Brikenstein, V. L. Broude, and A. G. Lavrushko, Pis'ma Zh. Eksp. Teor. Fiz. **17**, 472 (1973) [JETP Lett. **17**, 339 (1973)].
- <sup>8</sup>O. S. Avanesjan, V. A. Benderskii, V. Kh. Brikenstein, V. L. Broude, L. I. Korshunov, A. G. Lavrushko, and I. I. Tartakovskii, Mol. Cryst. Liq. Cryst. **29**, 165 (1974).
- <sup>9</sup>O. S. Avanesyan, V. A. Benderskii, V. Kh. Brikenstein, V. L. Broude, A. G. Lavrushko, and I. I. Tartakovskii, Kvantovaya Elektron. (Moscow) **4**, No. 4 (1977) [Sov. J. Quantum Electron. **7**, No. 4 (1977)].
- <sup>10</sup>V. A. Benderskii, V. Kh. Brikenstein, V. L. Broude, and A. G. Lavrushko, Solid State Commun. **15**, 1235 (1974).
- <sup>11</sup>A. V. Bree and L. E. Lyons, J. Chem. Soc. (Lond.) 2262 (1956).
- <sup>12</sup>P. Goursot, H. L. Girdnar, and E. F. Westrum, J. Phys. Chem. **74**, 2638 (1970).
- <sup>13</sup>A. A. Ovchinnikov, Zh. Eksp. Teor. Fiz. **57**, 2137 (1969) [Sov. Phys. JETP **30**, 1160 (1970)].
- <sup>14</sup>V. M. Agranovich, Teoriya eksitonov (Exciton Theory), Nauka, 1968, (a) Ch. 10, (b) Ch. 2, § 9.
- <sup>15</sup>T. D. Lee, K. Huang, and C. N. Yang, Phys. Rev. **106**, 1135 (1957).

Translated by J. G. Adashko

## Measurement of the electron temperature and density distributions in the plasma in the TM-3 Tokamak installation by the method of laser radiation scattering

V. V. Sannikov

(Submitted February 23, 1976)  
Zh. Eksp. Teor. Fiz. **72**, 119-126 (January 1977)

Electron temperatures of 0.15-1.2 keV have been measured at plasma densities  $\bar{n}_e = 6 \times 10^{12} - 6 \times 10^{13} \text{ cm}^{-3}$  under stable discharge conditions in the TM-3 Tokamak installation by the method of Thomson scattering. The electron temperature and density distributions along the plasma column radius have been obtained for different plasma parameters. The variation in time of the plasma-electron density and temperature profiles has been measured in one of the standard regimes ( $H_z = 22 \text{ kOe}$ ,  $J = 50 \text{ kA}$ ,  $\bar{n}_e = 6 \times 10^{13} \text{ cm}^{-3}$ ). The diamagnetic and laser measurements have been compared.

PACS numbers: 52.55.Gb, 52.70.Kz, 52.25.Lp

### 1. INTRODUCTION

The application of the technique of laser probing of a plasma in installations of the Tokamak type has allowed the accumulation of a large quantity of information about the local density,  $n_e$ , and temperature,  $T_e$ , of the electrons in the plasma column.<sup>[1-6]</sup> Of indubitable interest is the problem of the measurement of the distributions  $T_e(r)$  and  $n_e(r)$  on the TM-3 Tokamak installation, whose operating conditions allow the variation of the plasma parameters in a wide range of values. However, the small transverse dimensions of the diagnostic port on the installation limit considerably the transmission of the collection optics, and make it impossible for a diaphragm and a trap to be mounted for the purpose of suppressing the parasitic light scattered from the windows and walls of the vacuum chamber. On account of this, the fraction of the parasitic scattered light in the TM-3 facility attains an appreciable value. It becomes necessary to prepare the apparatus for Thomson scattering with appreciable suppression of the parasitic background.

In the experiment we used a polychromator assembled

on the basis of the high-transmission MDR-2 diffraction monochromator<sup>[7]</sup> with a selective ruby filter. The filter, which was 12 mm thick, was cut from a ruby crystal (with a chromium concentration in parts by weight in the blend of 0.5). Absorption in ruby depends on the orientation of the electric vector of the incident radiation relative to the optical axis of the crystal.<sup>[8]</sup> The filter was mounted in front of the entrance slit of the polychromator in such a way that the optical axis of the crystal was perpendicular to the polarization of the scattered light. Maximum absorption in the ruby line,  $R_1$ , is realized in this case. It was possible to reduce the intensity of the  $\lambda_0 = 6943 \text{ \AA}$  parasitic line, scattered from the windows and walls of the vacuum chamber, by a factor of more than  $10^2$  with the aid of the selective ruby filter.

The experiment was performed under stable discharge conditions in the Tokamak in the case when the stability safety factor had a value  $q > 3$ .

### 2. THE EXPERIMENTAL SETUP

A schematic diagram of the experiment is shown in Fig. 1. Scattered light from a  $0.2\text{-cm}^3$  plasma volume